

## Improvement evaluation of subgrade layer under geogrid-reinforced aggregate layer by finite element method

Wen-Chao Huang<sup>1,\*</sup>

Received: March 2013, Revised: January 2014, Accepted: January 2014

### Abstract

When geogrid reinforcement is used as a treatment method for improving soft subgrade as a roadway foundation, a top layer of subgrade is usually excavated and backfilled with geogrid-reinforced aggregates. This treatment method produces an adequate platform for the planned roadway construction site, where heavy traffic loading is constantly moving. This paper presents a quantitative assessment of subgrade improvement by geogrid reinforcement based on numerical modelling and parametric studies. First of all, the preliminary numerical models were verified by comparing the analysis results with previous studies. Secondly, the major numerical models in this study were assumed to be a simplified simulation of a geogrid-reinforced two-layer system with an aggregate layer above a subgrade layer. The numerical models were applied a quasi-static loading and unloading cycle, in order to monitor the permanent deformation at the surface of the models. Afterwards, thickness of aggregate layer, and subgrade CBR values were varied in order to summarize the outcomes of each case. This approach makes it possible to quantify the effects of geogrid reinforcement and aggregate material in terms of an enhanced California Bearing Ratio (CBR) of a single subgrade clay layer. Results have shown that when the aggregate thickness is up to 450mm, the contribution of enhanced CBR is mostly from aggregate material. However, when the aggregate thickness is about 150mm with a relatively weak subgrade material, the inclusion of geogrid material can contribute about 50% of the enhanced value.

**Keywords:** California bearing ratio, Finite element method, Geogrid reinforcement, Roadway, Subgrade layer, Aggregate layer.

### 1. Introduction

Road engineers often cite the problem of soft subgrade as one of the main causes of construction and maintenance difficulty. Aggregate placed on a poor foundation is prematurely subject to excessive permanent deformation during and after construction, and hence cannot achieve the expected performance. If, at the time of construction of the roadway and throughout the life of the pavement, moisture control such as drainage or drying is not practical or insufficient, the soft subgrade soil may become difficult to compact, unable to sustain heavy construction equipment traffic, or render compaction effort of the overlying aggregate ineffective. For pavement built on such a poor foundation, excessive permanent deformation, rutting, and cracking can be expected.

The treatment methods employed in areas with soft subgrades include excavation-substitution, stabilization with chemical additives and, more recently, mechanical reinforcement using geogrids.

A common practice is to combine the excavation-substitution and geogrid reinforcement techniques. In this approach, only the top layer of subgrade is excavated and then substituted with geogrid-reinforced aggregate. The tensile-resistant properties of the geogrid provide mechanical support and stiffness to the aggregate layer. This improves the subgrade response in terms of bearing capacity and plastic deformation. Analyzing this type of subgrade improvement under an applied surface load with geogrid and aggregate is a problem similar to that of analyzing reinforced unpaved roadway design. For practical reasons, it is desirable to develop a methodology capable of quantifying the mechanical improvement using a parameter common to reinforced and unreinforced subgrade layers.

Researchers have published several studies on the analysis and design of geosynthetic-reinforced unpaved roads. Previous models have been based on plastic equilibrium (Milligan et al., 1989), or on subgrade bearing capacity theories for geotextile reinforcement (Giroud and Noiray, 1981) and geogrid reinforcement (Giroud and Han, 2004). Milligan et al. (1989) proposed a design method for geosynthetic-reinforced unpaved roads. The analysis considered the plastic equilibrium of the aggregate layer and clay subgrade under a static load.

\* Corresponding author: wenchaoh@ncu.edu.tw  
1 Assistant Professor, Department of Civil Engineering, National Central University, Taiwan

While the aggregate material tends to slide outwards from the loading area, it is assumed that shear stresses developed at the base of the layer are balanced by the geosynthetic reaction; therefore only vertical stresses are transferred to the subgrade. This analysis also assumed that the geosynthetics as a reinforcement only provides enough friction along the interface between fill and clay subgrade so that the induced shear stress cannot be transferred to subgrade. Such a full shear stress transfer can be achieved when the geosynthetics was deformed significantly due to its low stiffness or excessive settlement that was occurred with existence of weak subgrade. Som and Sahu (1999) have also verified that even under such assumption (large deformation of geosynthetic may be required), the illustrated comparison shows well-matched behaviors between the results of analysis and experimental results. In addition, one of the most frequently used design methods for geotextile reinforced unpaved roads was suggested by Giroud and Noiray (1981). Based on the classical bearing capacity theory, the analysis consisted of two parts. First of all, the design thickness of the unreinforced case ( $h_0'$ ) under repeated loading is calculated based on existing empirical formulae that account for traffic. The performance of reinforced and unreinforced layers is then compared in order to estimate a reduction in aggregate layer thickness ( $\Delta h$ ) due to the reinforcement. The final design thickness with reinforcement is obtained by subtracting ( $\Delta h$ ) from ( $h_0'$ ). It is noted that, among the assumptions made, only the elastic limit bearing capacity of the subgrade soil is used when no reinforcement is present. In contrast, when geotextile reinforcement is used, it is assumed that the reinforced fill can undergo higher plastic deformations without failing, and the ultimate bearing capacity is used in this case. Another design approach that begins from considering the serviceability of the roadways was carried out by Giroud and Han (2004). The method is an evolution of an earlier method presented by Giroud et al. (1984) and has the same conceptual basis as the Giroud and Noiray (1981) method. The serviceability failure is defined when the rut depth exceeds the allowable rut depth which for example, 75mm. Since most of the rut depth comes from the deformation of the subgrade layer, the design approach is mainly focused on the determination of the vertical effective stress at the interface of the aggregate layer and subgrade layer. The cyclic loading on the behavior of unreinforced or reinforced roadways is also considered that the ability to distribute the stress from top of system will decrease in that it creates a local shear failure in the roadways and therefore after a number of cycles the system might reach failure.

All of the above design approaches relied on applications of theoretical derivation or experimental test results, however, the mechanical behavior and the sensitivity of each design parameter was seldom studied from a numerical analysis point of view. Not to mention a more convenient design approach considering only the subgrade layer with equivalent strength. Therefore in this study, numerical analysis employing finite element method (FEM) was conducted to explore the mechanical behavior

of the geogrid reinforced roadways. The numerical modeling employed elasto-plasticity for the aggregate and subgrade materials. Parametric studies using numerical models lead to an approach that treats the geogrid-reinforced mechanical effect as equivalent to the enhancement of the bearing capacity of the subgrade layer. The performance improvement can then be quantified as an equivalent increase in the subgrade California Bearing Ratio (CBR), which is compatible with current analysis methods in which no reinforcement is used.

## 2. Numerical Modeling

This study presents numerical models to analyze subgrade improvement using geogrid reinforcement and performed parametric studies. The models were formulated using finite element software, ABAQUS, to numerically simulate a two layer system (i.e., a subgrade layer overlaid by substituted aggregate base layer) including optional geogrid reinforcement at the interface of the two layer system. Fig. 1 shows a simplified axisymmetric geometry and surface loading pattern.

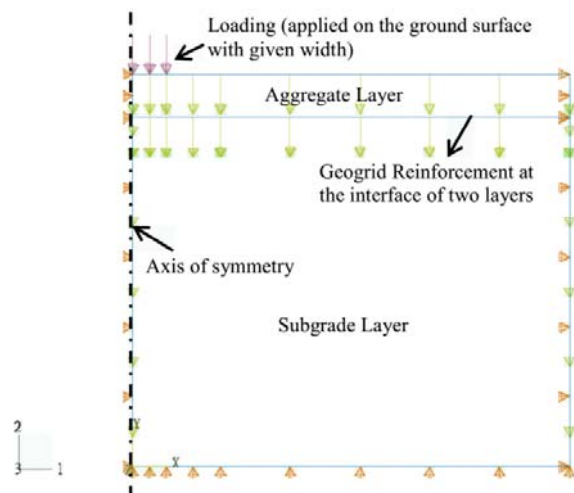


**Fig. 1** Illustration of basic numerical model with geogrid reinforcement (the arrows and triangles along the model boundary represent deformation direction and the boundary conditions)

An important phase in constructing a numerical model, prior to its application as an investigation tool, is to perform a comparative study with published studies that include physical or numerical model tests. This comparative study confirms the validity of the current modeling techniques. Thus, this study uses previous research results (Perkins, 1999, and Perkins and Edens, 2002, 2003) as a reference in the process of validating numerical models. Although the models presented in the literature have different configurations (such as 2D plane strain or axisymmetric conditions in numerical models and based on experimental setups), this study uses axisymmetric geometry models because they represent a suitable simplification of the problem. The simplified

model simulates the geogrid-reinforced roadway with a circular loading area on the ground surface, which is the same as the equivalent loading pattern proposed by Giroud and Han (2004), therefore in this study, the numerical model was also assumed to be axisymmetric. Other attributes, such as stratigraphy, boundary conditions, and material properties, were modeled as closely as possible to those mentioned in the literature for comparison. The following sections discuss the details of the numerical models.

### 2.1. Model layout and material properties

The validity of the numerical models in this study was examined by comparing with previous study results (Perkins, 1999, and Perkins and Edens, 2002, 2003). The geometry of the numerical model includes a 300mm thick aggregate layer that lies above a subgrade layer with thickness of 1125mm. The detailed discussion of the material properties follows.

Linear-elasticity was postulated for the geogrid reinforcement because the deformation required for mobilizing its strength is relatively small. Because axisymmetric solid elements were used to simulate the geogrid reinforcement, an equivalent homogenized modulus was determined based on actual biaxial geogrid reinforcement, as mentioned in the reference above.

The Drucker-Prager yield criterion was used for aggregate and subgrade layer because it is a common yield criterion for soils. The aggregate layer was considered as a purely frictional material whose resilient modulus  $M_R$  is related to the CBR of the aggregate material by the following empirical equation (AASHTO, 1993),

$$M_R(\text{kPa}) = 20690 \cdot \text{CBR}^{0.65} \quad (1)$$

Because some material properties in the references above are not readily available, the resilient modulus in the numerical modeling was assumed to be 100930 kPa because the common CBR of the aggregate material ranges from 11 to 12. The Poisson's ratio of the aggregate layer was set at 0.35 given that it is within the range of common granular materials. The friction angle of the aggregate layer is 30 degrees. The aggregate layer is cohesionless, however, to avoid singularity issues in the numerical models, the cohesion of the aggregate was assumed to be 1 kPa.

This study assumes that the subgrade layer is soft and saturated fine-grained soil. Because of the rapid loading-unloading cycle on the subgrade layer, the material was assumed to remain undrained. This was modeled in terms of total stress as an elastic-perfectly plastic behavior, where deformation occurs at a constant volume and yielding is controlled by undrained shear strength,  $c_u$ , with  $\phi_u=0$ . The CBR is usually used to characterize the subgrade strength through correlation with  $c_u$ . This study adopts this method using the empirical relationship between undrained shear strength and CBR (Giroud and Noiray, 1981),

$$c_u(\text{kPa}) = 30 \cdot \text{CBR} \quad (2)$$

The elastic modulus of the subgrade layer was estimated using the empirical relationship proposed by Huekelom and Klomp (1962),

$$E(\text{kPa}) = 10350 \cdot \text{CBR} \quad (3)$$

The Poisson's ratio of the subgrade layer was assumed to be 0.49 to account for the undrained condition under rapid loading-unloading process while remaining valid for numerical model analyses.

### 2.2. Consideration of soil and geogrid interface

The interaction between the geogrid and the adjacent soil layers, including aggregate and subgrade layers, is complex. This mechanism involves the upward movement of fine subgrade particles into the apertures of geogrid reinforcement. At the same time, the aggregate material becomes locked inside the grids and the geogrid apertures prevent the downward movement of the aggregate. With proper soil compaction efforts, geogrid reinforcement and the effect of aggregate interlocking with the geogrid can prevent the upward movement of subgrade particles. Based on the discussion above, the interface condition in a continuum mechanics model leads to the full interlocking of soil particles in grid apertures. In the finite element formulation, this translates to full adhesion and shear continuity at the interfaces between geogrid reinforcement, aggregate, and subgrade. However, this assumption is only valid when geogrid reinforcement is used because of the fact that interlocking behavior of geogrid reinforcement is more apparent comparing to other geosynthetic materials, such as geotextiles.

### 2.3. Surface loadings

For model verification purposes, the loadings in the models were chosen based on previous research. In the study performed by Perkins, loading was applied as uniformly-distributed on a circular area with a radius of 0.15m resulting in the maximum average pressure of 550kPa. These features represent, in a simplified way, the load induced by the tire of a 40kN single axle. This study simulates a quasi-static loading and unloading cycle by applying pressure increments with the maximum pressure mentioned above. This approach reveals the maximum stresses and deformation under peak load and permanent (i.e., plastic) deformation after unloading.

### 2.4. Boundary conditions of the numerical model

As shown in Fig. 1, the boundary condition along the centerline (or the symmetric axis) is assumed that only vertical displacement can take place, and the rotation or horizontal displacement cannot occur along this axis. Along the bottom of the model (i.e. the bottom of the subgrade layer), vertical displacement and rotation was not allowed, only horizontal displacement can occur along this

boundary. The thickness of the subgrade layer was assumed to be large enough such that the induced stress increment cannot propagate to the bottom of the model. The right boundary as shown in Fig. 1 was assumed to be able to deform only along the vertical direction. Horizontal displacement or rotation cannot occur along the right boundary. This is due to the sufficiently large width in the numerical models. The geometry as employed in the study can assure that the horizontal stress induced from the applied loading cannot extend to the right boundary. Finally no specific boundary conditions were applied on the ground surface in the numerical models.

### 3. Comparisons of Modeling Results

Before comparing the numerical results in this study and previous testing models, the regions with plastic strain were plotting for both unreinforced and reinforced cases. The inclusion of the geogrid reinforcement can actually

limit the development of the plastic deformation, as shown in Fig. 2 (unreinforced) and Fig. 3 (geogrid reinforced). In the aggregate layer of the reinforced case, the plastic region was smaller than that under unreinforced conditions. In the subgrade layer, the plastic region completely disappeared in the reinforced case. The induced plastic deformation in the reinforced case was also smaller in terms of numeric values in the aggregate layer. The results above show that geogrid reinforcement can reduce the potential for the development of plastic deformation in the subgrade layer. This study also compares the analyzed results with those in the literature based on the following three aspects: (1) variation of radial strain at the bottom of the aggregate layer, (2) variation of radial deformation of the geogrid reinforcement, and (3) variation of vertical strain along the center line of the loading area. Comparisons are discussed in the following sections.

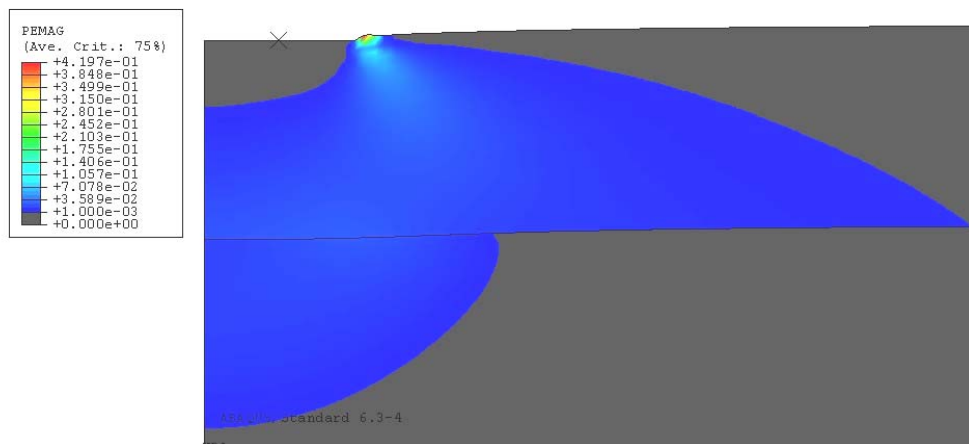


Fig. 2 Plastic region (PEMAG: the plastic strain) development in the unreinforced case

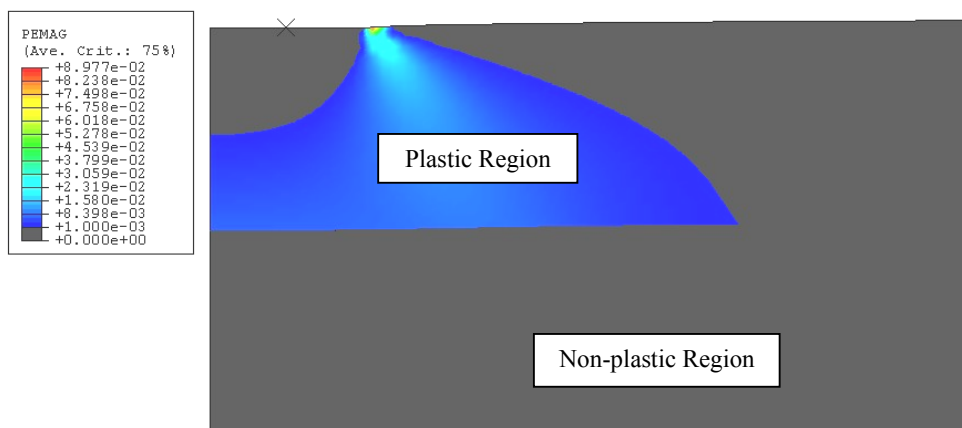


Fig. 3 Plastic region (PEMAG: the plastic strain) development in the reinforced (with geogrid) case

#### 3.1. Radial strain at the bottom of the aggregate layer

Fig. 4 shows the radial strain at the bottom of the aggregate layer. The radial strain under the condition with geogrid reinforcement is close to that in the literature

while in the unreinforced cases, the radial strains are similar, within a range of around 0.25% to 0.3%. These results show that the installation of geogrid reinforcement limits the radial strain along the bottom of the aggregate layer. The radial strain also changes sign after a distance of

approximately 0.3 m. This indicates that the lateral movement of the aggregate material extends outward to some distance outside the loading area. In this case, the lateral movement is approximately 0.3 m away from the center of the loading area.

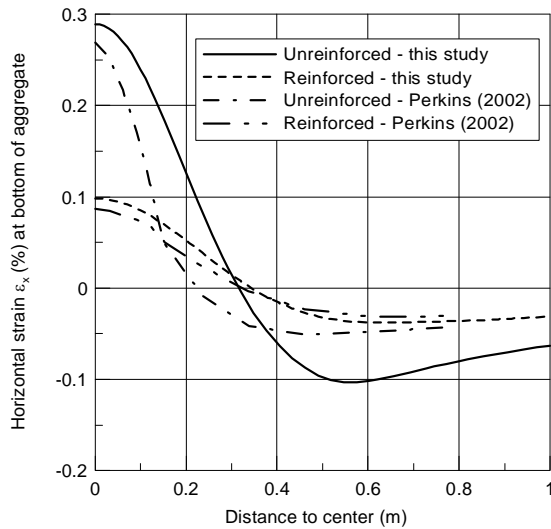


Fig. 4 Radial strain at bottom of the aggregate layer

### 3.2. Radial deformation of the geogrid reinforcement

The radial deformation of the geogrid reinforcement was obtained from numerical analysis and compared to the results reported in the literature (Fig. 5).

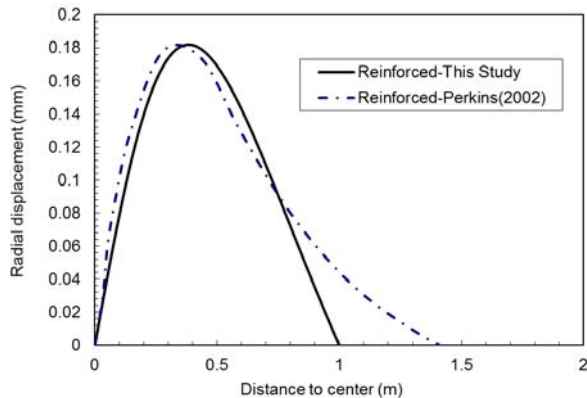


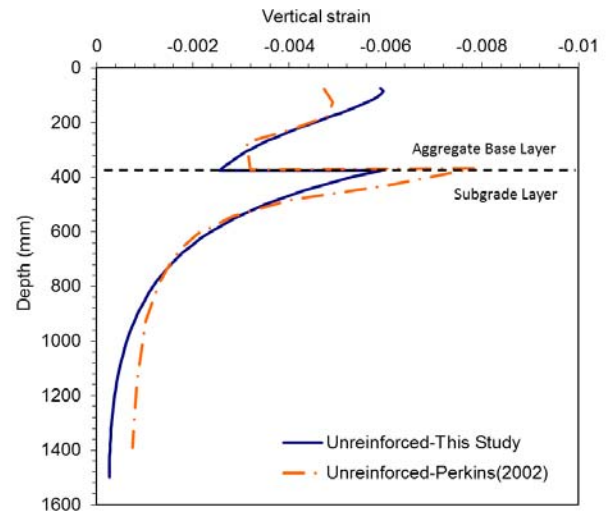
Fig. 5 Radial deformation of geogrid reinforcement

The radial deformation in both studies showed similar results. The maximum radial deformation of the geogrid reinforcement did not occur right below the center of the loading area (assuming that the numerical model is symmetric). Instead, the maximum radial displacement occurred at approximately three times the radius of the loading area away from the center of the loading plate, which is approximately 0.45 m. In addition, although the overall variation trend and the maximum geogrid radial displacement is very similar when comparing to the results proposed by Perkins (2002), due to different model

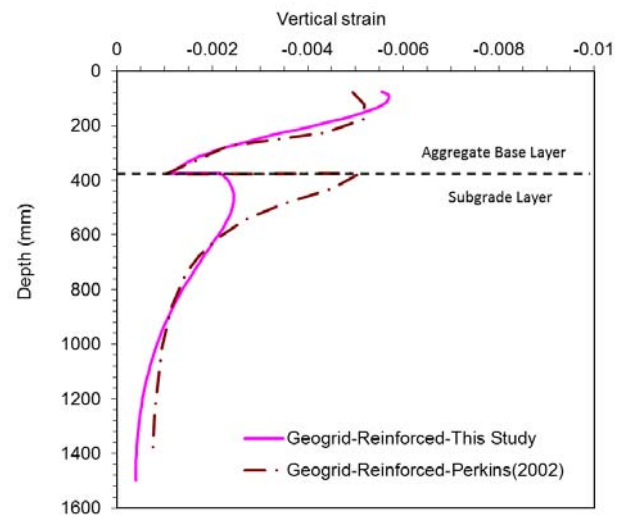
geometry applied in the numerical analysis, the variation of the trend close the right end of the model was slightly different.

### 3.3. Vertical strain along the centerline of the loading area within the soil mass

Figures 6 (a) and (b) show the variation of vertical strain in the soil mass in the unreinforced and reinforced cases, respectively. These figures show that the vertical strain decreased (negative sign denotes as downward deformation or compression) as it moved downward within the aggregate layer, showing the vertical strain attenuated within the aggregate layer.



(a)



(b)

Fig. 6 Variation of vertical strain along the centerline of loading in (a) unreinforced case and (b) geogrid reinforced case

However, the vertical strain at the top of the subgrade layer in both cases increased significantly compared to the vertical strain at the bottom of the aggregate layer. In the

case with geogrid reinforcement, the induced vertical strain in the subgrade layer was reduced significantly compared to the unreinforced case in both studies. This shows that the installation of geogrid limited the vertical strain development in the subgrade layer, and hence limited the propagation of plastic region, as mentioned in Fig. 2 and 3. There is a slight difference of the vertical strain at the top of the subgrade layer between the results in this study and that proposed by Perkins (2002), This may be due to different constitutive models of the material employed in the analyses, however, the overall trend and the range of the values are similar, therefore in this study, the Drucker-Prager yield criterion was employed for further parametric studies. The following sections discuss the analysis results and their application to the concept of subgrade equivalency.

#### 4. Parametric Study

This study adopts parametric analysis to understand the sensitivities of variables related to the reinforced two layer soil system similar to an unpaved roadway system. Before discussing the variables in the parametric studies for numerical models, this study chooses the following parameters as constants because their intrinsic characteristics can be controlled artificially. Preliminary analysis shows that these parameters are not major factors influencing the behavior of the two layer system. Parameters that are kept constant in the analyses include the material properties of the aggregate layer, the geometric layout of the numerical models, the loading conditions, and the location of the geogrid reinforcement (which is at the interface of the two soil layers). Furthermore, the thickness of the subgrade layer was kept constant at 1.125 m and the width of the numerical model (half of the numerical model) was 1.5m. As mentioned earlier, a loading of 550 kPa was applied on a circular loading area with a radius of 0.15 m. Other material properties that were kept constant are listed below:

Aggregate material: friction angle 30 degrees, cohesion 0 kPa, elastic modulus 100930 kPa.

Poisson's ratio 0.35, total unit weight 19kN/m<sup>3</sup>.

Subgrade layer: angle of internal friction angle 0 degree, total unit weight 19kN/m<sup>3</sup>.

The following sections discuss the parameters chosen as variables in the numerical model:

##### 4.1. Subgrade layer

Based on the results of the plastic region propagation discussed above, the undrained shear strength of the subgrade layer plays an important role in the performance of the two layer system. Preliminary model analysis also indicates that most of the soil deformation underneath the loading area came from the subgrade layer (Fig. 6). Therefore, the undrained shear strength of the subgrade layer is a critical factor in the two layer system in this parametric study. The discontinuity of the vertical strain at the interface of aggregate and subgrade layer in Fig. 6 indicated that the vertical displacement at the surface of

the subgrade layer is larger than that at the bottom of the aggregate layer. Since the induced stress at the interface is the same for the unreinforced case, with the higher stiffness of the aggregate layer, it is expected that the vertical strain in the aggregate layer is smaller. For the reinforced case, because the geogrid reinforcement has taken part of the vertical stress, the induced vertical strain in the subgrade layer is smaller compared to the unreinforced case, especially at the surface of subgrade layer. A gap or void may not be formed in the numerical model because the finite element mesh cannot be separated, however, in an actual case when the loading becomes large, a void or gap could be formed at the interface of aggregate and subgrade layer. When the above situation occurs, it is deemed failure of the geogrid reinforced system.

When subgrade layer is classified as very soft, the subgrade CBR is generally estimated to be smaller than 0.4, while for stiff subgrade, the CBR can range from 1.6 to 3.2. The CBR values employed in the parametric studies were thus chosen as 0.75, 1, 1.5, 2, 2.5, and 3 representing from soft (23 kPa) to stiff (90 kPa) subgrade materials. The required parameters of the subgrade layer were estimated through CBR by the empirical equations introduced previously.

##### 4.2. Thickness of aggregate layer

Installation of geogrid reinforcement can not only mitigate the plastic strain propagation potential, but also reduce the required thickness of the aggregate layer compared to the unreinforced case under the same surface deformation. To estimate the reduction of aggregate thickness caused by geogrid reinforcement in this study, four different values of aggregate thickness were chosen in the parametric studies: 100 mm, 150 mm, 300 mm, and 450 mm.

4.3 Properties of geogrid: This study assumes that the geogrid remains elastic under regular loading (550 kPa) because only a small deformation of the geogrid is necessary for it to develop its reinforcing effect in the two soil layer system. This study uses two different moduli for geogrid reinforcement: 205 MPa and 300 MPa. In both cases, the geogrid reinforcement was placed at the interface of the aggregate layer and subgrade layer.

#### 5. Results of Parametric Study

##### 5.1. Influence of subgrade CBR on plastic deformation

The parameter used to represent the model response is the plastic vertical deformation after incrementally increasing the load up to 550kPa and then decreasing it until complete unloading. The results shown here represent an aggregate layer thickness of 300 mm in Fig. 7 (a) and (b), for surface and interface plastic deformations, respectively. Other results with different aggregate thickness show similar trends. Plastic deformation at the surface of the aggregate layer and that at the interface is quite sensitive to the variations of CBR of subgrade layer,

especially in the range of soft to medium strength (CBR 0.75 to CBR 1.5). As the subgrade layer becomes softer (i.e., CBR values get smaller), the plastic deformation in both layers increases, especially in the absence of geogrid reinforcement. A comparison of the results in Figs. 7 (a) and (b) reveals that more than half of the plastic deformation occurs in the subgrade layer (aggregate vertical deformation is equal to the difference between surface and interface deformation). This confirms the decision to use the undrained shear strength of subgrade layer as the main variable in the parametric study. Geogrid reinforcement can reduce the plastic deformation in both layers effectively. Analyses with different aggregate thicknesses indicate that the thickness of the aggregate layer also affects the plastic deformation of the subgrade layer through the redistribution of vertical stress, as discussed in the following sections.

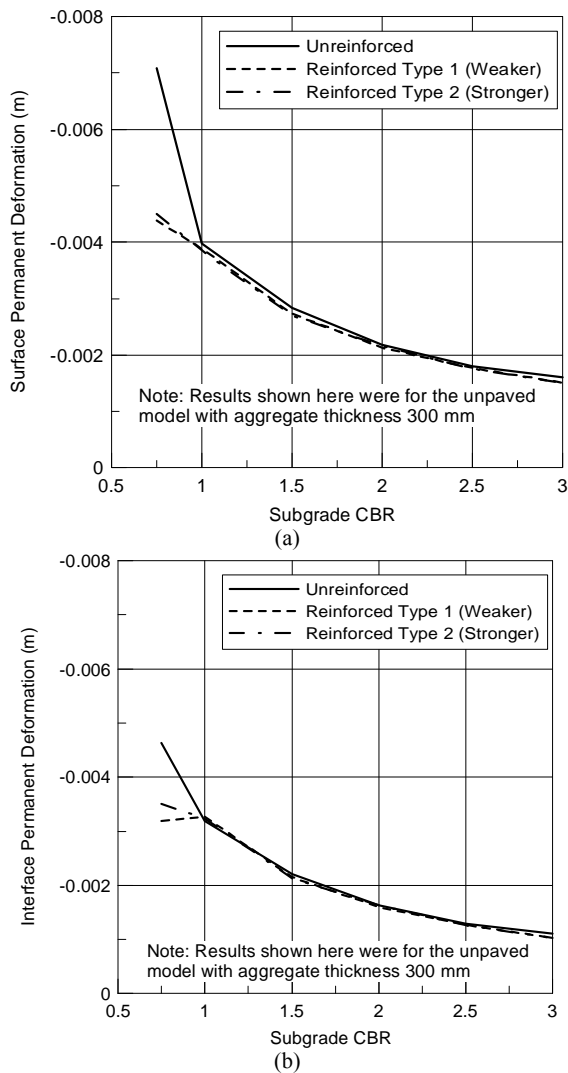


**Fig. 7** Plastic deformation V.S. subgrade CBR at (a) surface and (b) interface of a two layer system

5.2. Subgrade CBR and interface vertical stress

Previous research (Bourdeau, 1989) shows that the vertical stress at the top of the subgrade layer is reduced when geogrid reinforcement is present. This section discusses the reduction of vertical stress under different CBR values of the subgrade with the same aggregate layer thickness. Since the geogrid reinforcement shares part of the transferred vertical stress from the aggregate layer (Bourdeau, 1989), the required vertical stress to balance the system in the subgrade layer was hence reduced. Figs. 8 (a) and (b) show the advantages of geogrid reinforcement in terms of the reduction of vertical stress on the subgrade layer. As the CBR values increase, the induced vertical stress values also increase. Comparing the induced vertical stress under the unreinforced and reinforced cases, Fig. 8 (a) (CBR 0.75, the lowest CBR chosen for this parametric study) shows that the vertical stress reduction due to the geogrid reinforcement is approximately 12%.

Fig. 8 (b) (subgrade CBR 3.0) shows that the geogrid reinforcement did not have a noticeable effect on the reduction of induced vertical stress on the subgrade compared to the unreinforced case. As the CBR of the subgrade layer gets larger, the advantage (in terms of vertical stress reduction) of the geogrid reinforcement becomes smaller. The results of numerical modeling above indicate that the advantage of installation of geogrid reinforcement may not be as significant when the subgrade layer is relatively strong.

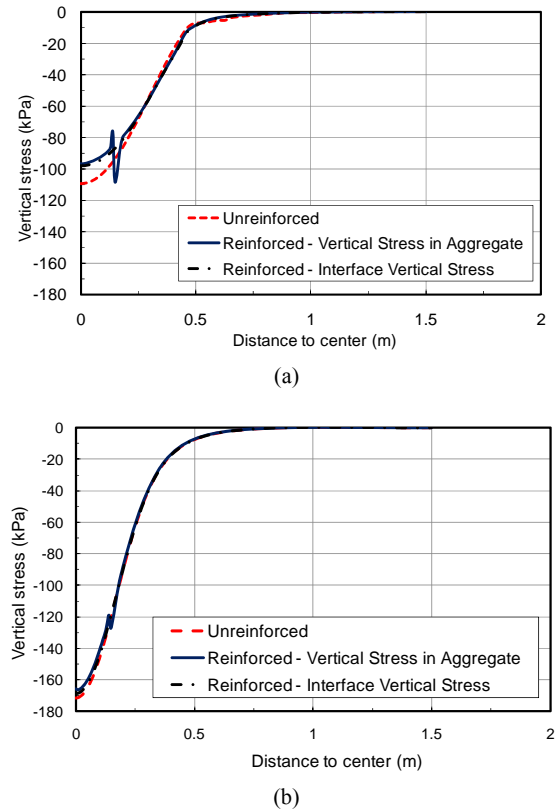


**Fig. 8** Vertical stress distribution at the top of the subgrade layer for subgrade (a) CBR 0.75 (b) CBR 3

### 5.3. Influence of aggregate thickness on plastic deformation of the aggregate layer and subgrade layer

As mentioned above, the thickness of the aggregate layer is also an important parameter affecting the behavior of the two layer system. When geogrid reinforcement is installed in a two layer system to achieve the same system performance when there is no geogrid reinforcement, the required aggregate thickness can be reduced because the effect of vertical stress attenuation to the top of the subgrade layer is replaced by the existence of geogrid reinforcement. The required aggregate thickness becomes smaller when geogrid reinforcement is used, resulting in less compaction effort to reach the same required compactness of the aggregate material and the subgrade layer. This section discusses the relationship between the thickness of aggregate layer and the plastic deformation of the two layer system. Specifically, the following discussion is based on the situation when the subgrade CBR is 1.5.

Figs. 9 (a) and (b) show the plastic vertical deformations of the aggregate surface and at the interface of the two layers, with subgrade CBR of 1.5, as a function of aggregate thickness. As expected, when the thickness of the aggregate layer increases, the amount of plastic deformation decreases dramatically for both layers. This trend confirms previous findings on the effect of aggregate substitution in subgrade improvement. This mechanism is well known as a load diffusion behavior through the aggregate layer, and results in an attenuated condition of interface stresses. For the subgrade CBR of 1.5 used in the example shown here, the benefit of increasing the aggregate thickness (comparing reinforced with unreinforced case) is less sensitive for large aggregate thicknesses (e.g., 300mm and thicker) than for thinner layers. Relatively thin aggregate layers with geogrid reinforcement show significant improvement for the two layer system. Both figures 9 (a) and (b) show that the plastic deformations are not significantly affected by the presence of geogrid reinforcement when the aggregate layer is thicker than 300mm, while significant reduction appears in presence of thinner layers. The tensile modulus of the geogrid reinforcement, within the range of values used in this study, has only a minor effect on the plastic deformation variation patterns. This may be due to the fact that the moduli were taken from the actual product information, and the difference between these two types of geogrid was not too significant, therefore by examining from the permanent (plastic) deformation after the loading was removed, it was expected that the deformation difference may not be too significant.

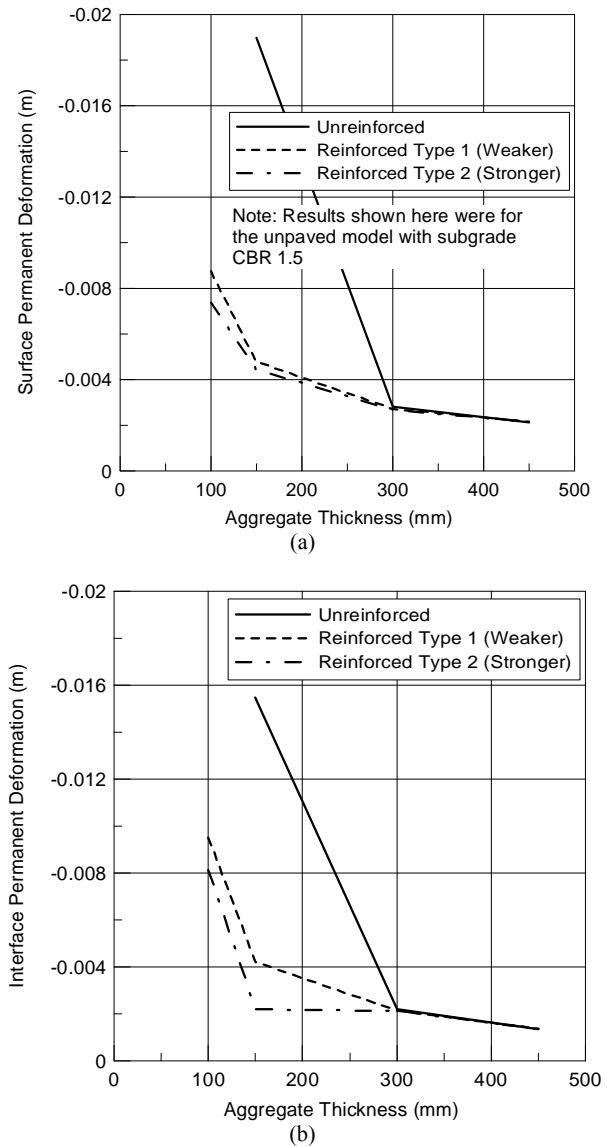


**Fig. 9** Plastic deformation V.S. aggregate thickness at (a) surface and (b) interface

The discussions about the mutual relationships among subgrade CBR values, aggregate thicknesses, and the plastic deformation of the two layer system reveals that the response of the two layer system is closely related to the subgrade CBR values and the thickness of the aggregate layer. Previous discussions only consider a certain value of subgrade CBR or a certain value of aggregate thickness. This study shows that the combination of subgrade CBR and the aggregate thickness have certain threshold combinations for the geogrid reinforcement to be most advantageous in terms of the plastic deformation on the surface of the two layer system. To obtain a comprehensive understanding of the mutual effects of subgrade CBR and aggregate thickness, this study presents the plastic deformation versus different subgrade CBR under different aggregate thickness (Fig. 10 (a), (b), (c), and (d)).

Figures 10 (a), (b), (c) and (d) show that the benefit of

increasing subgrade CBR at different aggregate thicknesses with geogrid reinforcements is no longer significant beyond certain subgrade CBR values. For example, in Figure 10 (c), as the CBR becomes larger than 1.0, the difference between unreinforced and reinforced is no longer apparent. According to this concept, Figure 11 shows a geogrid reinforcing threshold curve describing the usefulness of geogrid reinforcement under different combinations of subgrade CBR and aggregate thickness. Any subgrade CBR-aggregate thickness combination below this curve shows significant improvement when

using geogrid reinforcement at the interface. Because the threshold curve was obtained based on parametric studies within a certain ranges of subgrade CBR and aggregate thickness, this curve should not be extrapolated beyond the ranges of the parameters used in this study. This study also shows that the strength of geogrid reinforcement does not have a noticeable effect on vertical stress reduction. This might be because of the relatively smaller loading applied to the system. Stronger geogrid reinforcement might have advantages over weaker geogrid reinforcement under heavier loadings.

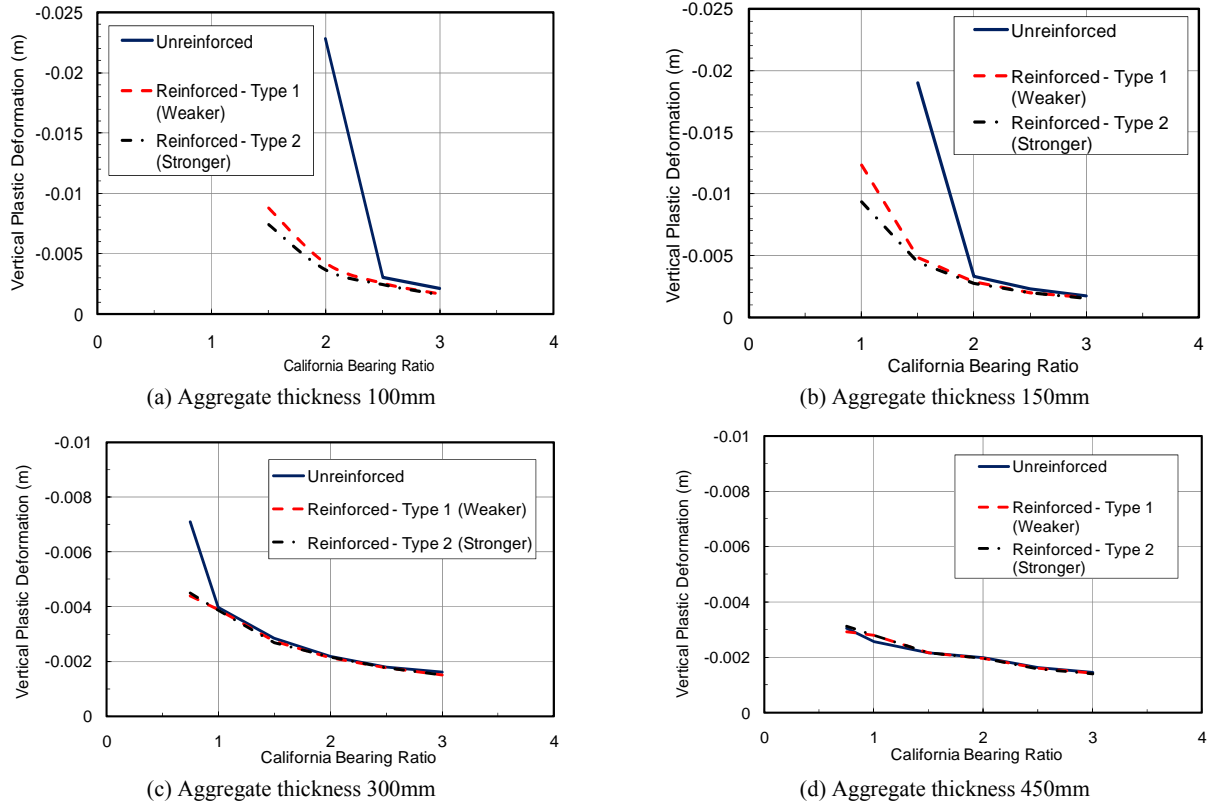


**Fig. 10** Vertical plastic deformation at the center of the loading area

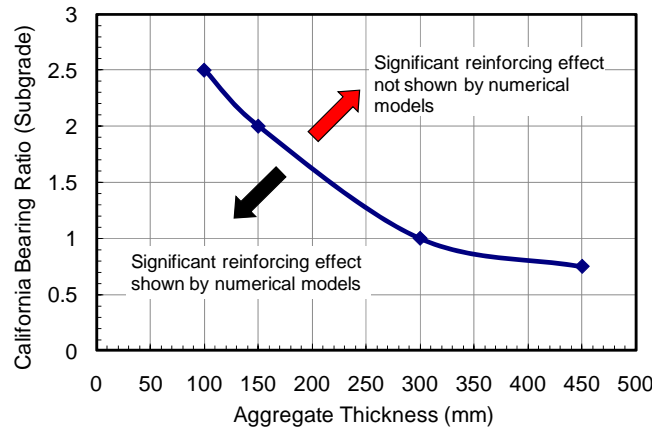


**Fig. 11** Geogrid-reinforcing threshold curve

## 6. Enhanced Subgrade CBR

### 6.1. Concept of equivalent subgrade

Based on the results of parametric studies, this study proposes a reinforcing threshold curve for preliminary evaluation of geogrid-reinforced two layer system as shown in Fig. 11. This section proposes the concept of equivalent subgrade CBR by considering different model layouts. Figs. 12 (a), (b), and (c) show three model configurations all with the same subgrade thickness. In case (a), the upper layer of subgrade was excavated and substituted with aggregate material, as shown in the upper hatched area. In case (b), the same aggregate substitution was attempted, but a layer of

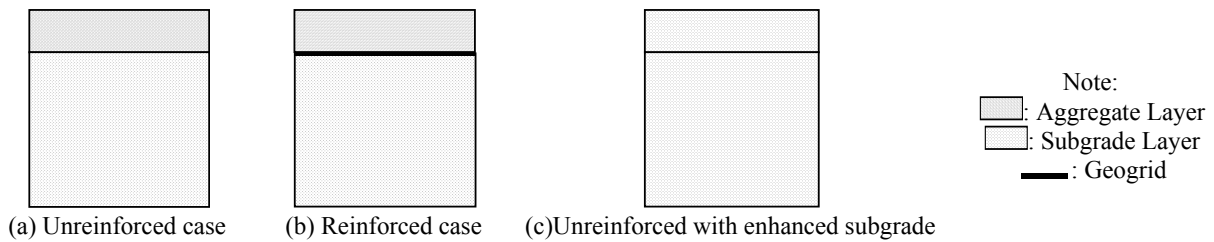


Fig. 12 Model layout for analysis of the concept of equivalent subgrade CBR

### 6.2. Synthesis of results in terms of enhanced subgrade CBR

This study uses a database of the parametric study results to quantify the improvement using the concept of enhanced subgrade CBR. Figure 13 shows the analysis for a 100mm-thick aggregate layer. For example, when the actual subgrade CBR is 1.5, the permanent deformation is 7 mm with aggregate substitution and geogrid reinforcement. If no reinforcement is used and only aggregate substitution is used, as in case (a), the subgrade CBR in case (a) must be 2.4 to achieve the same plastic vertical deformation as in case (b). If no aggregate or reinforcement is used, as in case (c), the CBR must be as high as 3.3 to achieve the same performance. For this particular set of data, the combined effects of aggregate and geogrid reinforcement enhanced the subgrade CBR from its original value of 1.5 to 3.3, whereas the geogrid contributes 0.9 to the total CBR improvement compared to cases (a) and (b).

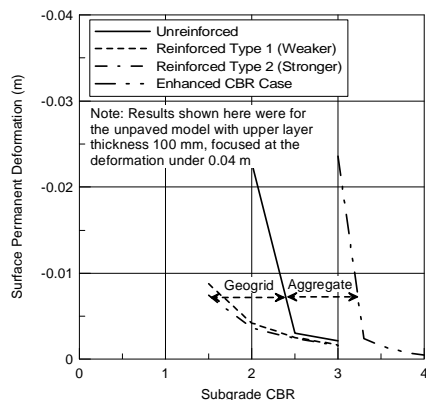


Fig. 13 Enhanced subgrade CBR analysis for aggregate layer thickness of 100mm

geogrid reinforcement was installed at the interface. Case (c) only includes subgrade soil with no aggregate or geogrid reinforcement. Assume that all three cases, when subjected to the same loading, produce the same plastic vertical deformation at the surface. If the subgrade CBR is the controlling parameter, the above situation can occur only if the subgrade CBR in case (c) is higher than cases (a) and (b). Assuming that the geogrid reinforcement is effective, this also means that the subgrade CBR in case (a) should be higher than that in (b) to obtain the same performance. In other words, aggregate substitution and geogrid reinforcement in case (b) have an effect on plastic surface deformation equivalent to the system performance when enhancing the subgrade CBR in case (a) and case (c).

Figs. 14 (a) through (d) show similar presentation of the results at different thicknesses of the aggregate layer considered in the parametric studies. Table 1 summarizes the analysis results for subgrade CBR values starting from 1.5 with aggregate thicknesses of 100mm and 150mm, and for subgrade CBR starting from 0.75 with aggregate thicknesses of 300mm and 450mm. The lower part of Table 1 provides the individual contributions of the geogrid and the aggregate layer (in percentage of the total subgrade CBR enhancement). When thin layers of aggregate are present in the system, the contribution from the geogrid reinforcement compared to the overall improvement is significant (50% of the subgrade improvement comes from geogrid reinforcement). However, the geogrid reinforcement becomes the sole source of improvement as the aggregate layer becomes thicker. The results presented in Table 1 suggest that when geogrid reinforcement is installed in a two layer system (especially when the subgrade CBR is lower than 2 after evaluating from Fig. 11), it is more economically beneficial when aggregate layer thickness is 100 to 150 mm.

**Table 1** Equivalent subgrade CBR under different reinforcing scenarios

Concept of Enhanced Subgrade Equivalency Approach	Aggregate Thickness (mm)			
	100	150	300	450
Actual Subgrade CBR	1.5	1.5	0.75	0.75
Equivalent CBR	Unreinforced	2.4	1.9	0.9
	Reinforced	3.3	3.25	3.3
Enhanced CBR Contributed by Geogrid and Aggregate	1.8	1.75	2.55	2.55
Enhanced CBR Contributed by Geogrid Only	0.9 (50%)	0.4 (23%)	0.15 (6%)	0 (0%)
Enhanced CBR Contributed by Aggregate Only	0.9 (50%)	1.35 (77%)	2.4 (94%)	2.55 (100%)

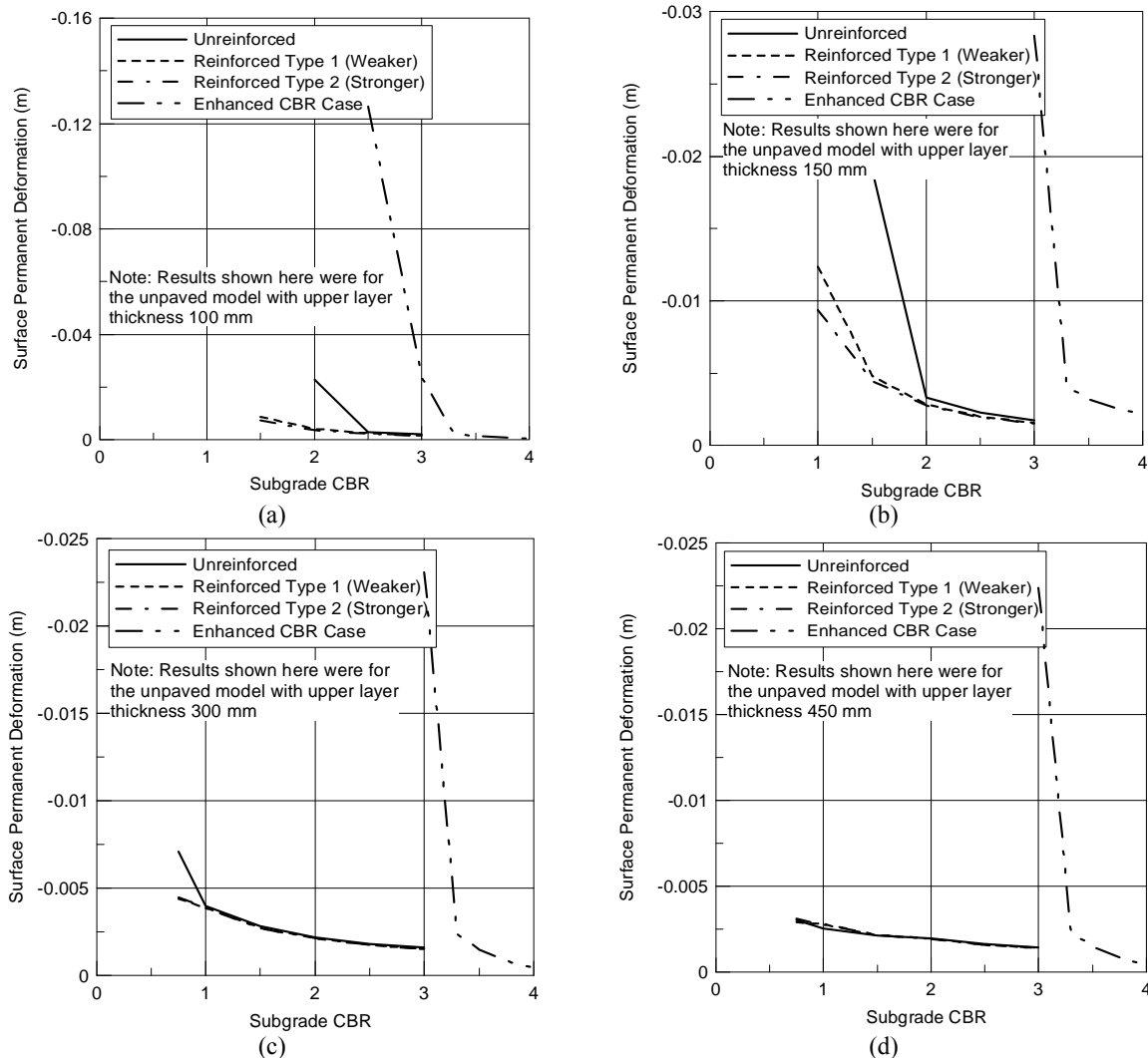


Fig. 14 Enhanced subgrade CBR analyses for different aggregate layer thicknesses

## 7. Conclusions

This study uses finite element analysis of a two-layer soil system reinforced at the interface and subjected to

surface applied loading to simulate the behavior of soft subgrade when its upper layer has been excavated and substituted with geogrid-reinforced aggregate. This numerical procedure was validated by comparison with an earlier established model.

This study also investigates the sensitivity of the model

response to the most critical parameters through a series of computations. Plastic deformation was significantly greater when both the subgrade CBR and the aggregate layer thickness decreased. There seems to be an optimal arrangement of these parameters for the two layer soil system to be effective. When the subgrade CBR is relatively high or the aggregate layer is thick, further subgrade improvement from geogrid reinforcement is marginal or non-existent.

The results of this study show that the benefit obtained by placing the geogrid and aggregates to improve a soft subgrade can be quantified as an equivalent enhancement of the subgrade CBR. Results indicate that the analysis of geogrid-reinforced two layer system is most effective when the aggregate layer thickness is approximately 100 to 150 mm. Under these circumstances, the aggregate material and the geogrid reinforcement can contribute about 50% improvement of the subgrade material. When the aggregate layer is thicker, such as 300 mm, the geogrid reinforcement may not be as efficient when it is compared to the improvement contributed by the aggregate material.

**Acknowledgments:** This study is part of a project (No. SPR-2459) supported by the Joint Transportation Research Program and administered by the Indiana Department of Transportation and Purdue University. The author is grateful to the inputs and support from the above organizations.

## References

- [1] AASHTO Guide for Design of Pavement Structures, American Association of State Highway and Transportation Officials, Washington, DC, 1993.
- [2] Bourdeau PL. Modelling of membrane action in a two-layer reinforced soil, *Computers and Geotechnics*, 1989, Vol. 7, pp. 19-36.
- [3] Giroud JP, Noiray L. Geotextile-reinforced unpaved road design, *Journal of Geotechnical Engineering*, 1981, No. GT9, Vol. 107, pp. 1233-1254.
- [4] Giroud JP, Ah-Line C, Bonaparte R. Design of unpaved roads and trafficked areas with geogrids, *Proceedings of Polymer Grid Reinforcement*, London, UK, 1984, pp. 116-127.
- [5] Giroud JP, Han J. Design method for geogrid-reinforced unpaved roads. I. Development of design method, *Journal of Geotechnical and Geoenvironmental Engineering*, 2004, No. 8, Vol. 130, pp. 775-786.
- [6] Giroud JP, Han J. Design method for geogrid-reinforced unpaved roads. II. Calibration and Applications, *Journal of Geotechnical and Geoenvironmental Engineering*, 2004, No. 8, Vol. 130, pp. 787-797.
- [7] Huekelom W, Klomp AJG. Dynamic testing as a means of controlling pavements during and after construction, *Proceedings of the First International Conference on the Structural Design of Asphalt Pavements*, Ann Arbor, Michigan, 1962, pp. 667-685.
- [8] Milligan GWE, Jewell RA, Houlsby GT. A new approach to the design of unpaved roads-part I, *Ground Engineering*, 1989, pp. 25-29.
- [9] Milligan GWE, Jewell RA, Houlsby GT, Burd HJ. A new approach to the design of unpaved roads-part II, *Ground Engineering*, 1989, pp. 37-42.
- [10] Perkins SW. Mechanical Response of Geosynthetic-Reinforced Flexible Pavements, *Geosynthetics International*, 1999, No. 5, Vol. 6, pp. 347-382.
- [11] Perkins SW, Edens MQ. Finite Element and Distress Models for Geosynthetic-Reinforced Pavements, *International Journal of Pavement Engineering*, 2002, No. 4, Vol. 3, pp. 239-250.
- [12] Perkins SW, Edens MQ. A design model for geosynthetic-reinforced pavements, *International Journal of Pavement Engineering*, 2003, No. 1, Vol. 4, pp. 37-50.
- [13] Som N, Sahu RB. Bearing capacity of a geotextile-reinforced unpaved road as a function of deformation: a model study, *Geosynthetics International*, 1999, No. 1, Vol. 6, pp. 1-17.